Numer. Math. Theor. Meth. Appl.
doi: 10.4208/nmtma.2011.m1027

Vol. **4**, No. 4, pp. 505-524
November 2011

Simulations of Shallow Water Equations by Finite Difference WENO Schemes with Multilevel Time Discretization

Changna Lu[1,*] and Gang Li[2]

[1] *College of Mathematics & Physics, Nanjing University of Information Science & Technology, Nanjing, Jiangsu 210044, P.R. China.*
[2] *School of Mathematical Science, Qingdao University, Qingdao 266071, P. R. China.*

Received 7 September 2010; Accepted (in revised version) 10 February 2011

Available online 7 November 2011

Abstract. In this paper we study a class of multilevel high order time discretization procedures for the finite difference weighted essential non-oscillatory (WENO) schemes to solve the one-dimensional and two-dimensional shallow water equations with source terms. Multilevel time discretization methods can make full use of computed information by WENO spatial discretization and save CPU cost by holding the former computational values. Extensive simulations are performed, which indicate that, the finite difference WENO schemes with multilevel time discretization can achieve higher accuracy, and are more cost effective than WENO scheme with Runge-Kutta time discretization, while still maintaining nonoscillatory properties.

AMS subject classifications: 65M10, 78A48

Key words: Multilevel time discretization, weighted essentially non-oscillatory schemes, shallow water equations, Runge-Kutta method, high order accuracy.

1. Introduction

In this paper, the finite difference weighted essential non-oscillatory (WENO) schemes with linear multilevel time discretizations are used to simulate discontinuous flows of the shallow water equations with source terms. The numerical solutions are compared with those of WENO schemes with Runge-Kutta time discretizations. We will be mainly addressing on cost CPU time and resolution.

WENO schemes were firstly developed from essential non-oscillatory (ENO) scheme, which share many advantages with and usually perform better than TVD or TVB schemes,

*Corresponding author. *Email addresses:* luchangna@nuist.edu.cn (C. Lu), gangli1978@163.com (G. Li)

because they use an adaptive stencil trying to obtain information from the smoothest regions. ENO schemes started with the classic paper of Harten, *et al*, in 1987 [8, 9]. WENO schemes use a convex combination of all candidate stencils instead of the one used as in the original ENO. The first WENO scheme was constructed in 1994 by Liu et al. [13] for the third order finite volume version in one space dimension. Then the third and the fifth order finite difference WENO schemes in multi-space dimensions were constructed. With a general framework for the design of smoothness indicators and nonlinear weights [11], higher order WENO finite difference schemes up to the eleventh order were designed in [3], very high order WENO schemes up to the seventeenth order were developed in [7], and WENO schemes were generalized to triangle meshes [10]. WENO improves upon ENO in robustness, better smoothness of fluxes, better steady convergence, better provable convergence properties, and more efficiency [17].

WENO is a procedure of spatial discretization; namely, it is a procedure to approximate the spatial derivative terms. It forms a very important class of high accuracy numerical methods [11,13], leading to a class of high order finite difference or finite volume methods for hyperbolic conservation laws [2, 20]. They give sharp, non-oscillatory discontinuity transitions and at the same time provide high order accurate resolutions for the smooth part of the solution [4, 21].

For time-dependent problems, we need accuracy of time discretization as well. There are mainly two different approaches to approximate the time derivative [14, 18]. One way is via the classical Lax-Wendroff procedure, which relies on converting all the time derivatives in a temporal Taylor expansion into spatial derivatives, then discretizing the spatial derivatives, so it is also called the Taylor type. The approach can produce the same high order accuracy with a smaller effective stencil. The other way is to use a high order ODE solver, such as Runge-Kutta method or multilevel type. The approach has the advantages of simplicity in concept and in coding and they are easily generalizable to multidimensional problems. Runge-Kutta method is commonly used, but the method costs more CPU time, as for every time step it must iterate k times for the k-th order Runge-Kutta method. Multilevel time discretization methods can make full use of given information with spatial discretization. Stencils of multilevel time discretization are more compact than that of Runge-Kutta methods, since we communicate only with immediate neighbors of cell i to computed u_i^{n+1} from u_i^n, and the CFL number of multilevel method is smaller than that of Runge-Kutta method, while they need the same memory of the cells. Linear multilevel methods are the most commonly used in multilevel procedures.

In this paper, the fifth order WENO finite difference schemes with multilevel type time discretization are used to solve the one-dimensional and two-dimensional shallow water equations. We follow the ideas of Jiang and Shu about the WENO schemes [11], Rogers *et al.* [16] and Xing and Shu [19] about the balance of the flux and the source terms of shallow water equations, and linear multilevel time discretization. This paper is organized as follows. In Section 2, we describe the discretization and numerical method of the shallow water equations. Numerical examples are given to demonstrate the advantages of maintaining high order accuracy, the resolution and cost effective of the constructed schemes in Section 3. Concluding remarks are included in Section 4.

2. Description of numerical model and numerical method

2.1. The governing equations

The two-dimensional conservative unsteady shallow water equations are

$$U_t + F(U)_x + G(U)_y = S(U), \tag{2.1}$$

with

$$U = [D, uD, vD]^T, \qquad F(U) = [uD, u^2D + gD^2/2, uvD]^T,$$
$$G(U) = [vD, uvD, v^2D + gD^2/2]^T,$$

and the source terms

$$S(U) = [0, -gDb_x, -gDb_y]^T, \tag{2.2}$$

where D is the total water depth, u and v are the depth-averaged velocities in the $x-$ and $y-$ directions, respectively, t is the time; g is the gravitational acceleration, b_x and b_y are the bed slopes stresses, b is the bottom function. Other terms could also be added into source terms in order to include effects such as friction on the bottom and Coriolis terms.

We write the shallow water equations in quasi-linear form as follows

$$U_t + A(U)U_x + B(U)U_y = S(U), \tag{2.3}$$

where

$$A(U) = \frac{\partial F}{\partial U} = \begin{pmatrix} 0 & 1 & 0 \\ c^2 - u^2 & 2u & 0 \\ -uv & v & u \end{pmatrix}, \qquad B(U) = \frac{\partial G}{\partial U} = \begin{pmatrix} 0 & 0 & 1 \\ -uv & v & u \\ c^2 - v^2 & 0 & 2v \end{pmatrix},$$

$c = \sqrt{gD}$ is the propagation speed of the shallow water wave. The eigenvalues of Jabobians A and B are

$$\lambda(A) = u - c, u, u + c, \qquad \lambda(B) = v - c, v, v + c;$$

respectively. The corresponding right and left eigenvectors of Jacobin A and B as follow:

$$R_A = \begin{pmatrix} 1 & 0 & 1 \\ u - c & 0 & u + c \\ v & 1 & v \end{pmatrix}, \qquad L_A = \begin{pmatrix} \frac{u+c}{2c} & -\frac{1}{2c} & 0 \\ -v & 0 & 1 \\ -\frac{u-c}{2c} & \frac{1}{2c} & 0 \end{pmatrix}, \tag{2.4}$$

$$R_B = \begin{pmatrix} 1 & 0 & 1 \\ u & 1 & u \\ v - c & 0 & v + c \end{pmatrix}, \qquad L_B = \begin{pmatrix} \frac{v+c}{2c} & 0 & -\frac{1}{2c} \\ -u & 1 & 0 \\ -\frac{v-c}{2c} & 0 & \frac{1}{2c} \end{pmatrix}. \tag{2.5}$$

2.2. Description of the fifth order finite difference WENO schemes

We solve the spatial derivative of the shallow water equations using the finite difference formulation. In this section, we give a short overview for one-dimensional scalar hyperbolic conservation law as (2.6),

$$u_t + f(u)_x = 0. \tag{2.6}$$

The two-dimensional cases procedure in a dimension-by-dimension fashion, for more details, we refer to [11].

Denote $I_i = [x_{i-\frac{1}{2}}, x_{i+\frac{1}{2}}]$ be the ith cell, centered on x_i, we assume that the grid points are uniform with $\Delta x = x_{i+1} - x_i$. For a finite difference scheme, we evolve the point value u_i at mesh points x_i in time. The spatial derivative $f(u)_x$ is approximated by a conservative flux difference

$$f(u)_x|_{x_i} \approx \frac{1}{\Delta x}(\hat{f}_{i+\frac{1}{2}} - \hat{f}_{i-\frac{1}{2}}).$$

For a $(2r-1)$th order WENO scheme, the numerical flux $\hat{f}$ is computed through r neighboring point values $f^{\pm}$ by $\hat{f} = \hat{f}^{+} + \hat{f}^{-}$. We use Lax-Friedrichs splitting as

$$f^{\pm}(u) = \frac{1}{2}\Big(f(u) \pm \alpha u\Big),$$

where α is taken as $\alpha = \max_u |f'(u)|$.

Let $f_i = f^{+}(u_i)$. For example, the fifth order WENO scheme ($r = 3$), the 3 numerical fluxes are given by

$$\begin{aligned}
\hat{f}^{(0)}_{i+\frac{1}{2}} &= \frac{1}{3}f_i + \frac{5}{6}f_{i+1} - \frac{1}{6}f_{i+2},\\
\hat{f}^{(1)}_{i+\frac{1}{2}} &= -\frac{1}{6}f_{i-1} + \frac{5}{6}f_i + \frac{1}{3}f_{i+1},\\
\hat{f}^{(2)}_{i+\frac{1}{2}} &= \frac{1}{3}f_{i-2} - \frac{7}{6}f_{i-1} + \frac{11}{6}f_i.
\end{aligned}$$

The next is to compute the smoothness indicators and the nonlinear weights. The $(2r-1)$th order WENO flux is a convex combination of all these r numerical fluxes

$$\hat{f}^{+}_{i+\frac{1}{2}} = \sum_{m=0}^{r-1} \omega_m \hat{f}^{(m)}_{i+\frac{1}{2}}.$$

The nonlinear weights ω_m are defined in the following way:

$$\omega_m = \frac{\alpha_m}{\sum_{s=0}^{r-1}\alpha_s}, \qquad \alpha_s = \frac{d_s}{(\varepsilon + \beta_s)^2},$$

where d_s are the linear weights which yield $(2r-1)$th order accuracy, β_s are the so-called "smoothness indicators", which measure the smoothness of those polynomials. ε is a small

positive constant used to avoid the denominator to become zero and is typically taken as 10^{-6}. For the fifth order WENO scheme, the linear weights d_s are given by

$$d_0 = \frac{3}{10}, \quad d_1 = \frac{3}{5}, \quad d_2 = \frac{1}{10},$$

and the smoothness indicators β_s are given by

$$\begin{aligned}
\beta_0 &= \frac{13}{12}(f_i - 2f_{i+1} + f_{i+2})^2 + \frac{1}{4}(3f_i - 4f_{i+1} + f_{i+2})^2,\\
\beta_1 &= \frac{13}{12}(f_{i-1} - 2f_i + f_{i+1})^2 + \frac{1}{4}(f_{i-1} - f_{i+1})^2,\\
\beta_2 &= \frac{13}{12}(f_{i-2} - 2f_{i-1} + f_i)^2 + \frac{1}{4}(f_{i-2} - 4f_{i-1} + 3f_i)^2.
\end{aligned}$$

$\hat{f}^-$ can be computed with mirror symmetry procedure to that of $\hat{f}^+_{i+1/2}$ with respect to $x_{i+1/2}$. For the shallow water equations, we use the local characteristic decomposition, which is more robust than a component by component. The right eigenvectors and the left eigenvectors of the Jacobian A and B and Roe's average are needed for the local characteristic decomposition.

2.3. Balance of the flux and the source terms

Here we adopt the ideas of Rogers *et al.* [16] about the balance of the flux and the source terms, they presented an algebraic technique for balancing the flux gradients and the source terms. The numerical imbalance is eradicated by reformulating the governing matrix hyperbolic system of conservation laws in terms of deviations away from an unforced but separately specified equilibrium state. Thus, balancing is achieved by the incorporation of this extra physical information and bypasses conventional numerical treatments of the imbalance.

The vector of conserved variables U is given by

$$U = U^{eq} + \tilde{U}, \tag{2.7}$$

where $\tilde{U}$ is the deviation of U from the equilibrium or still water value such that $\partial U^{eq}/\partial t = 0$. Actually, for still water values, the shallow water convenient properties $\zeta = u = v = 0$, and

$$U^{eq} = [h, 0, 0]^T, \qquad \tilde{U} = U - U^{eq} = [\zeta, uD, vD]^T,$$

in which ζ is the free surface elevation above the still level $h + b$, ζ is still water height, $D = \zeta + h$ is the total water depth. The shallow water equations are transformed to

$$\frac{\partial \tilde{U}}{\partial t} + \frac{\partial [F(U) - F(U^{eq})]}{\partial x} + \frac{\partial [G(U) - G(U^{eq})]}{\partial y} = S(U) - \frac{\partial (F(U^{eq}))}{\partial x} - \frac{\partial (G(U^{eq}))}{\partial y}, \tag{2.8}$$

$$\tilde{U}_t + \tilde{F}(U)_x + \tilde{G}(U)_y = \tilde{S}(U), \tag{2.9}$$

with

$$\tilde{U} = [\zeta, uD, vD]^T, \qquad \tilde{F} = [uD, u^2D + g(\zeta^2 + 2h\zeta)/2, uvD]^T,$$
$$\tilde{G} = [vD, uvD, v^2D + g(\zeta^2 + 2h\zeta)/2]^T,$$
$$\tilde{S}(U) = [0, -g\zeta b_x, -g\zeta b_y]^T. \tag{2.10}$$

We can see that the Jacobian matrixes $\tilde{A}(U)$ and $\tilde{B}(U)$ of (2.9) are same as $A(U)$ and $B(U)$ of (2.1), and the discretization of the equations (2.9) is similar to that of (2.1).

The approach taken in the paper for some examples chosen are to use the still water level as the datum h. It is perfectly reasonable to choose a fixed horizontal datum elsewhere, and derive the balanced hyperbolic equations using a stage-discharge approach. The scheme reduces to the original WENO scheme describe in the previous section when the bottom is flat. In the thesis, straight forward treatments of the modified source terms with its point values are used.

The scheme reduces to the original WENO scheme describe in the previous section when the bottom is flat. In order to keep the high order accuracy of the WENO scheme for the shallow water equations with source terms, inspired by Xing [19], we procedure the source terms as follows. For the two-dimensional shallow water equations, we perform the same WENO procedure to approximate the source terms, namely, we use the local characteristic decomposition and the same nonlinear weights to the vector $[0, b, 0]^T$ in $x-$ direction and $[0, 0, b]^T$ in $y-$ direction to approximate the derivative in source terms, in other words, one half of the derivative in source term is approximated by the operator obtained from the computation of f^+ as described in Section 2.2, and the other half is computed by the operator obtained from the computation of f^- with biased stencils, so the approximation to source terms is also a fifth order accuracy, and the method is suit to problems with discontinuous bottom topography or the nonexistence derivative of bottom function.

2.4. Description of a class of time discretizations

In this section, we describe shortly the construction of a class of multilevel time discretizations with the one-dimensional scalar hyperbolic conservation law as (2.6).

Denote Δt be the time step, $t^{n+1} = t^n + \Delta t$, let u^n be the approximation of the point values $u(t^n)$, the linear multilevel time discretization, which are the most commonly used in multilevel type, for $u_t = L(u)$ as follows:

$$u^{n+1} = \sum_{k=0}^{m} \alpha_k u^{n-k} + h \sum_{k=-1}^{m} \beta_k L(u^{n-k}), \tag{2.11}$$

where $h \approx \Delta t$, $\beta_{-1} \neq 0$ means its a implicit formula, $\beta_{-1} = 0$ means its a explicit formula. Taylor expansion or numerical integral methods are commonly used to construct linear multilevel time discretization formula. The main idea of Taylor expansion method is as follows: use Taylor expansion to every terms of linear multilevel formula at t_n, the right

hand terms in (2.11), compare it with Taylor expansion of $u(t_{n+1})$ at t_n and make those anterior terms the same to fix parameters of α_k and β_k.

We list some frequently-used linear multilevel formulas as follows:
If $m = 2$:

$$u^{n+1} = u^n + \frac{h}{12}\Big(23L(u^n) - 16L(u^{n-1}) + 5L(u^{n-2})\Big), \tag{2.12}$$

which is the third order explicit Adams formula;

$$u^{n+1} = u^n + \frac{h}{24}\Big(9L(u^{n+1}) + 19L(u^n) - 5L(u^{n-1}) + L(u^{n-2})\Big), \tag{2.13}$$

which is the fourth order implicit Adams formula.
If $m = 3$:

$$u^{n+1} = u^n + \frac{h}{24}\Big(55L(u^n) - 59L(u^{n-1}) + 37L(u^{n-2}) - 9L(u^{n-3})\Big), \tag{2.14}$$

which is the fourth order explicit Adams formula;

$$u^{n+1} = u^n + \frac{h}{720}\Big(251L(u^{n+1}) + 646L(u^n) - 264L(u^{n-1}) + 106L(u^{n-2}) - 19L(u^{n-3})\Big), \tag{2.15}$$

which is the fifth order implicit Adams formula.

In the same way, we can get linear multilevel formulas as follows:
Milne formula:

$$u^{n+1} = u^{n-3} + \frac{4h}{3}\Big(2L(u^n) - L(u^{n-1}) + 2L(u^{n-2})\Big); \tag{2.16}$$

Hamming formula:

$$u^{n+1} = \frac{1}{8}\Big(9u^n - u^{n-2}\Big) + \frac{3h}{8}\Big(L(u^{n+1}) + 2L(u^n) - L(u^{n-1})\Big); \tag{2.17}$$

Simpson formula:

$$u^{n+1} = u^{n-1} + \frac{h}{3}\Big(L(u^{n+1}) + 4L(u^n) + L(u^{n-1})\Big). \tag{2.18}$$

It is difficult to use implicit formula with WENO scheme for hyperbolic equation, since shocks may be generated. A great point of multilevel type is need of other initial value except for initial data, which is not need for single step type of Lax-Wendroff type. We can get initial values of multilevel scheme using single step methods with the same order accuracy, such as Runge-Kutta method. In this paper, the third order TVD Runge-Kutta method is used for the initial values of the third order explicit formula, the fourth order Runge-Kutta method is used for the initial values of the fourth order explicit formula to keep high order accuracy. The third order TVD version and the fourth order version for $u_t = L(u)$ are given respectively by

$$\begin{aligned} u^{(1)} &= u^n + \Delta t L(u^n), \\ u^{(2)} &= \frac{3}{4}u^n + \frac{1}{4}u^{(1)} + \frac{1}{4}\Delta t L(u^{(1)}), \\ u^{n+1} &= \frac{1}{3}u^n + \frac{2}{3}u^{(2)} + \frac{2}{3}\Delta t L(u^{(2)}); \end{aligned} \tag{2.19}$$

and

$$
\begin{aligned}
u^{(1)} &= u^n + \frac{1}{2}\Delta t L(u^n),\\
u^{(2)} &= u^n + \frac{1}{2}\Delta t L(u^{(1)}),\\
u^{(3)} &= u^n + \Delta t L(u^{(2)}),\\
u^{n+1} &= \frac{1}{3}\Big(-u^n + u^{(1)} + 2u^{(2)} + u^{(3)}\Big) + \frac{1}{6}\Delta t L(u^{(3)}).
\end{aligned}
\tag{2.20}
$$

3. Numerical results

In this section, we perform numerical experiments to test the performance of the fifth order finite difference WENO schemes with different linear multilevel time discretization developed in the previous section, such as the third order explicit Adams multilevel type and the fourth order explicit Adams multilevel type. In this section, we mainly give the results of WENO scheme with the third order explicit Adams multilevel time discretization for the shallow water equations to save space, as the Figures are similar. We denote the module with WENO5-AD3, and compare the results with that of the fifth order WENO schemes with the third order TVD Runge-Kutta time discretization, which we denote with WENO5-RK3, addressing on the important issue of cost CPU time and relevant efficiency, both one-dimensional and two-dimensional shallow water equations are studied. We also use the abbreviations of WENO5-AD4 and WENO5-RK4.

For CPU time comparison, all the computations are performed on a personal computer, Core (TM) 2 Duo CPU P8600 @ 2.4 GHz with 4 GB ram. In our numerical experiments, the gravitation constant is taken as 9.812 m/s^2; the small positive constant in the WENO weight formula is taken as $\varepsilon = 10^{-6}$, except for the special test. We did stability analysis of linear WENO5-AD3 and WENO5-AD4 for $u_t + u_x = 0$ using standard Fourier analysis, and the CFL number of WENO5-AD3 and WENO5-AD4 are about 0.52 and 0.31, respectively. so the CFL number is taken as 0.35 for WENO5-AD3 schemes, 0.21 for WENO5-AD4 schemes, and 0.8 for WENO5-RK3 and WENO5-RK4 schemes, which are about 80% of the biggest numbers. Uniform meshes are used.

Example 3.1. An one-dimensional accuracy test over a sinusoidal hump [5, 13]. To check the order accuracy of the schemes for a smooth solution of the one-dimensional shallow water equations, we use the same test in [19]. In the domain $[0, 1]$, the bottom topography is given by

$$b(x) = \sin^2(2\pi x),$$

the initial data are given by

$$
\begin{aligned}
D(x,0) &= 5 + e^{\cos(2\pi x)},\\
(Du)(x,0) &= \sin(\cos(2\pi x)).
\end{aligned}
$$

We take the still water height h as $h = 5 - b(x)$. We compute up to time $t = 0.1$ s when there is no shocks in the solution, with a 2-periodic boundary conditions. The reference solution is computed with the same scheme and 25600 points, since the exact solution is unknown.

Table 1: L^1 errors and numerical orders of accuracy for the one-dimensional order test, WENO5-AD3 and WENO5-RK3 using N space points.

N	WENO5-AD3				WENO5-RK3			
	D		Du		D		Du	
	L^1 error	order	L^1 error	order	L^1 error	order	L^1 error	order
25	1.458E-2		1.180E-1		1.457E-2		1.180E-1	
50	2.093E-3	2.80	2.220E-2	2.41	2.093E-3	2.80	2.219E-2	2.41
100	3.285E-4	2.67	2.935E-3	2.92	3.285E-4	2.67	2.935E-3	2.92
200	2.308E-5	3.83	2.022E-4	3.86	2.308E-5	3.83	2.022E-4	3.86
400	9.346E-7	4.63	8.081E-6	4.65	9.349E-7	4.63	8.083E-6	4.64
800	3.206E-8	4.87	2.758E-7	4.87	3.207E-8	4.87	2.759E-7	4.87
1600	1.038E-9	4.95	8.947E-9	4.95	1.040E-9	4.95	8.967E-9	4.94

Table 2: L^∞ errors and numerical orders of accuracy for the one-dimensional order test, WENO5-AD3 and WENO5-RK3 using N space points.

N	WENO5-AD3				WENO5-RK3			
	D		Du		D		Du	
	L^∞ error	order	L^∞ error	order	L^∞ error	order	L^∞ error	order
25	7.038E-2		6.264E-1		7.034E-2		6.261E-1	
50	1.743E-2	2.01	1.685E-1	1.89	1.743E-2	2.01	1.685E-1	1.89
100	4.324E-3	2.01	3.664E-2	2.20	4.323E-3	2.01	3.664E-2	2.20
200	5.147E-4	3.07	4.743E-3	2.95	5.147E-4	3.07	4.743E-3	2.95
400	2.885E-5	4.16	2.554E-4	4.22	2.884E-5	4.16	2.554E-4	4.22
800	1.034E-6	4.80	8.788E-6	4.86	1.034E-6	4.80	8.787E-6	4.86
1600	3.260E-8	4.99	2.767E-7	4.99	3.256E-8	4.99	2.764E-7	4.99

In Table 1, the L^1 numerical errors and orders of accuracy by WENO5-AD3 and WENO5-RK3 for water depth D and the discharge Du are displayed for comparison, where N is the number of points. The L^∞ numerical errors and orders of accuracy by WENO5-AD3 and WENO5-RK3 are shown in Table 2. We can see that the fifth order accuracy are almost achieved for both WENO5-AD3 and WENO5-RK3 schemes; they produce similar numerical errors and orders of accuracy.

In Fig. 1, we give the L^1 and L^∞ numerical errors for D and Du and CPU time when space points numbers are N=25, 50, 100, 200, 400, 800, 1600, and Log scale for both numerical errors and CPU time are used. We can see that the line of WENO5-AD3 always at the bottom of the line of WENO5-RK3, which means that to get the same numerical

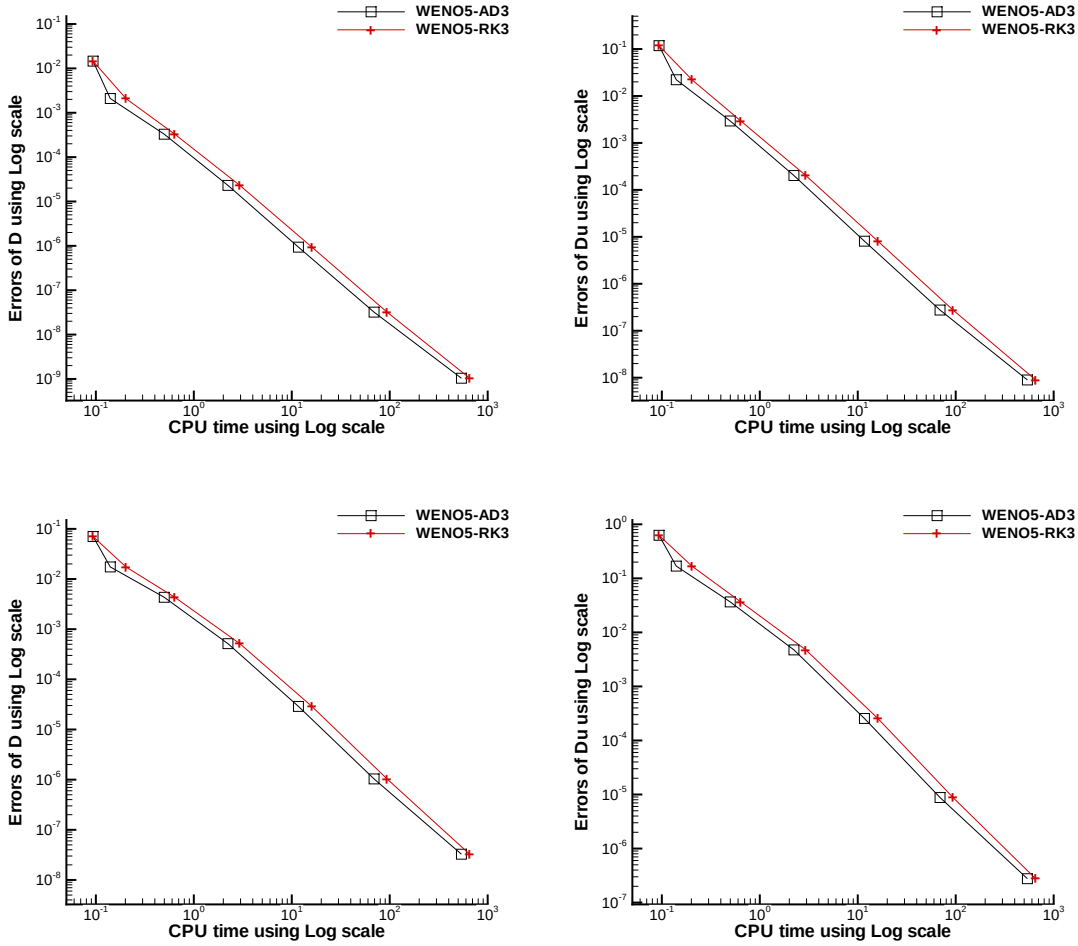

Figure 1: $Log_{10}^{Numericalerrors}$ and $Log_{10}^{CPUtime}$ by WENO5-AD3 and WENO5-RK3 with $N = 25, 50, 100, 200, 400, 800, 1600$ cell points for the one-dimensional order test. Top: L^1 errors. Bottom: L^∞ errors.

error, WENO5-RK3 costs more CPU time. Moreover, WENO5-AD3 has more superiority when the cell number is bigger, about 80% of WENO5-RK3 for the total CPU time.

The numerical errors and orders of WENO5-AD4 and WENO5-RK4 are similar, the cost CPU time of WENO5-AD4 is 59.8s, while that of WENO5-RK4 is 65.7s.

For this test, we also simulated flows with WENO5 and the fourth order explicit Milne formula. The results of orders of accuracy are given in Tables 3 and 4, and the numerical errors and the cost CPU time used are displayed in Fig. 2. We can see that the results are similar to that of WENO5-AD4 and better than that of WENO5-RK4.

Table 3: L^1 errors and numerical orders of accuracy for the one-dimensional order test, WENO5-Milne and WENO5-RK4 using N space points.

N	WENO5-Milne				WENO5-RK4			
	D		Du		D		Du	
	L^1 error	order	L^1 error	order	L^1 error	order	L^1 error	order
25	1.459E-2		1.181E-1		1.458E-2		1.180E-1	
50	2.097E-3	2.80	2.222E-2	2.41	2.093E-3	2.80	2.220E-2	2.41
100	3.285E-4	2.67	2.936E-3	2.92	3.287E-4	2.67	2.936E-3	2.92
200	2.307E-5	3.83	2.022E-4	3.86	2.308E-5	3.83	2.022E-4	3.86
400	9.304E-7	4.63	8.040E-6	4.65	9.350E-7	4.63	8.085E-6	4.64
800	3.178E-8	4.87	2.719E-7	4.89	3.207E-8	4.87	2.759E-7	4.87
1600	1.189E-9	4.74	9.557E-9	4.83	1.040E-9	4.95	8.967E-9	4.94

Table 4: L^∞ errors and numerical orders of accuracy for the one-dimensional order test, WENO5-Milne and WENO5-RK4 using N space points.

N	WENO5-Milne				WENO5-RK4			
	D		Du		D		Du	
	L^∞ error	order	L^∞ error	order	L^∞ error	order	L^∞ error	order
25	7.050E-2		6.271E-1		7.038E-2		6.257E-1	
50	1.745E-2	2.01	1.686E-1	1.89	1.744E-2	2.01	1.685E-1	1.89
100	4.332E-3	2.01	3.671E-2	2.20	4.323E-3	2.01	3.664E-2	2.20
200	5.150E-4	3.07	4.746E-3	2.95	5.149E-4	3.07	4.745E-3	2.95
400	2.891E-5	4.16	2.559E-4	4.21	2.885E-5	4.16	2.555E-4	4.22
800	1.042E-6	4.79	8.854E-6	4.85	1.034E-6	4.80	8.786E-6	4.86
1600	3.468E-8	4.91	2.936E-7	4.91	3.256E-8	4.99	2.764E-7	4.99

Example 3.2. Test for the exact C-property. In this test case [15,19], the bottom is defined with

$$b(x) = 5e^{-\frac{2}{5}(x-5)^2}, \qquad x \in [0,1],$$

the initial water height is defined as $D(x) = 1 - b(x)$, and the initial velocity u is defined as zero. The surface should remain flat. The terminal time is taken as $t = 0.5s$.

We take the still level h as $h = 1 - b(x)$. In Table 5, L^1 and L^∞ errors of water height D and the discharge Du for WENO5-AD3 and WENO5-RK3 are displayed respectively with different meshes. The results obviously confirm the theoretical predictions. The accuracy is quite satisfactory. We run 100 times as the CPU time, the cost CPU time is 17.84s for WENO5-AD3, and 23.82s for WENO3-RK3 when space points number is 500. The corresponding CPU time is 31.02s for WENO5-AD4 and 33.47s for WENO5-RK4.

Example 3.3. Dam break on a flat bed. The dam-break problem is the most common test to evaluate the performance of shock capturing schemes in shallow flows, see, e.g. [15].

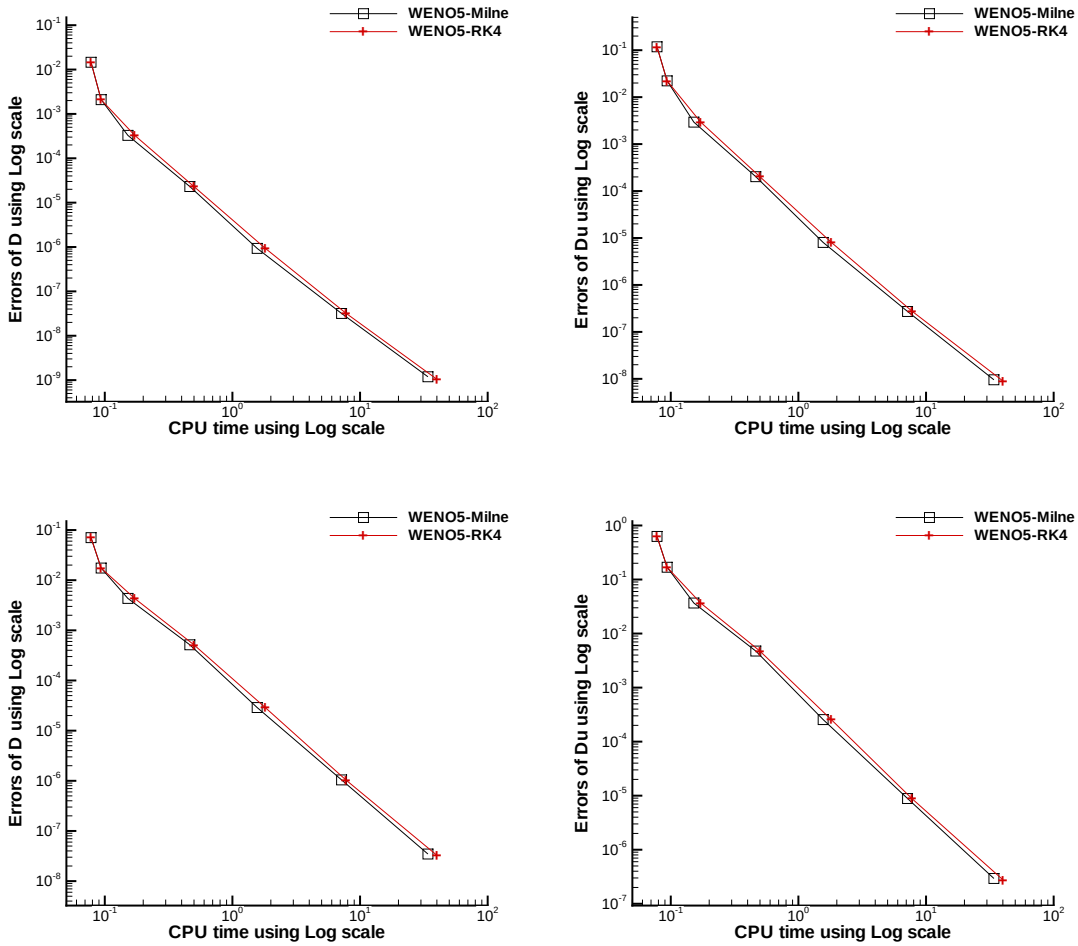

Figure 2: $Log_{10}^{Numericalerrors}$ and $Log_{10}^{CPUtime}$ by WENO5-Milne and WENO5-RK4 with $N = 25, 50, 100, 200, 400, 800, 1600$ cell points for the one-dimensional order test. Top: L^1 errors. Bottom: L^∞ errors.

The bottom is flat $b(x) = 0$ and the initial conditions are taken as:

$$D(x,0) = \begin{cases} D_1, & x < 0, \\ D_2, & x \geq 0, \end{cases} \qquad (Du)(x,0) = 0. \tag{3.1}$$

We take the computational domain as $[-1,1]$, $D_1 = 1$m and $D_2 = 0.1$m. The simulation is performed up to time $t = 0.1$s.

The water depth D and the discharge Du using the WENO5-AD3 and WENO5-RK3 schemes on a mesh with 200 points and exact solution are plotted in Fig. 3, which show very good agreement with the exact solution [6], and no spurious oscillations occurred. We

Table 5: L^1 and L^∞ errors for the stationary solution, WENO5-AD3 and WENO5-RK3 using N space points.

N	WENO5-AD3				WENO5-RK3			
	D		Du		D		Du	
	L^1	L^∞	L^1	L^∞	L^1	L^∞	L^1	L^∞
500	6.82E-16	1.78E-15	5.89E-15	3.04E-14	1.24E-15	3.55E-15	7.25E-15	3.03E-14
200	1.47E-15	5.33E-15	1.51E-14	6.59E-14	2.75E-15	7.11E-15	2.19E-14	5.56E-14
100	6.57E-16	3.55E-15	6.14E-15	1.85E-14	1.03E-15	3.55E-15	1.46E-14	3.02E-14

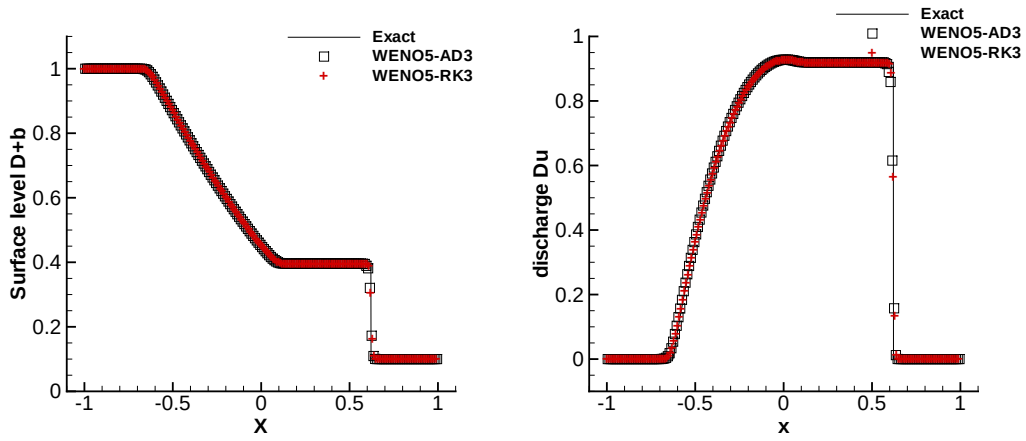

Figure 3: Dam break on a flat bed by WENO5-AD3 and WENO5-RK3. Left: water depth; Right: discharge.

run 100 times as the CPU time for every program, the CPU time is 1.83s for WENO5-AD3, 2.26s for WENO5-RK3, while the CPU time is 2.85s for WENO5-AD4, 3.11s for WENO5-RK4.

Example 3.4. A small perturbation of steady-state water. This is a classical example to show the capability of the proposed scheme for the perturbation of the stationary state [19]. In the domain $[0,2]$, the bottom topography is given by the function

$$b(x)=\begin{cases} 0.25\Big(\cos(10\pi(x-1.5))+1\Big), & 1.4\le x\le 1.6,\\ 0, & \text{otherwise,}\end{cases}$$

the initial data are given by

$$D(x,0)=\begin{cases} 1-b(x)+\beta, & 1.1\le x\le 1.2,\\ 1-b(x), & \text{otherwise,}\end{cases}\qquad (Du)(x,0)=0.$$

Here the small pulse $\beta = 0.001$. Fig. 4 displays the surface level by WENO-AD3 and WENO5-AD4 with $\varepsilon = 10^{-6}$ and $\varepsilon = 10^{-12}$, which verified the results of the relative bigger ε have oscillation, WENO5-RK3 and WENO5-RK4 are also sensitive to the value of ε. For this small pulse problem, we take $\varepsilon = 10^{-12}$ in the weight formulas for WENO schemes, as 10^{-6} is not small enough relatively, and maybe interfere the resolution of small pulse. Fig. 5 displays the left and right-going waves of the small pulse by WENO5-AD3 and WENO5-RK3. Reference solutions are computed by WENO5-RK3 with 3000 points. We can clearly see that there are no spurious numerical oscillations produced by both WENO5-AD3 scheme and WENO5-RK3 scheme with 200 points, and the results are comparable

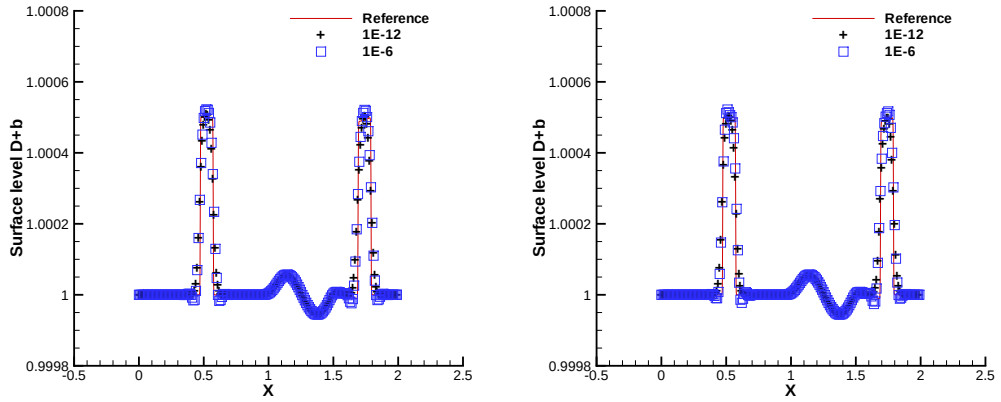

Figure 4: Results of surface level with $\varepsilon = 1E-6$ and $\varepsilon = 1E-12$. Left: by WENO5-AD3; Right: by WENO5-AD4.

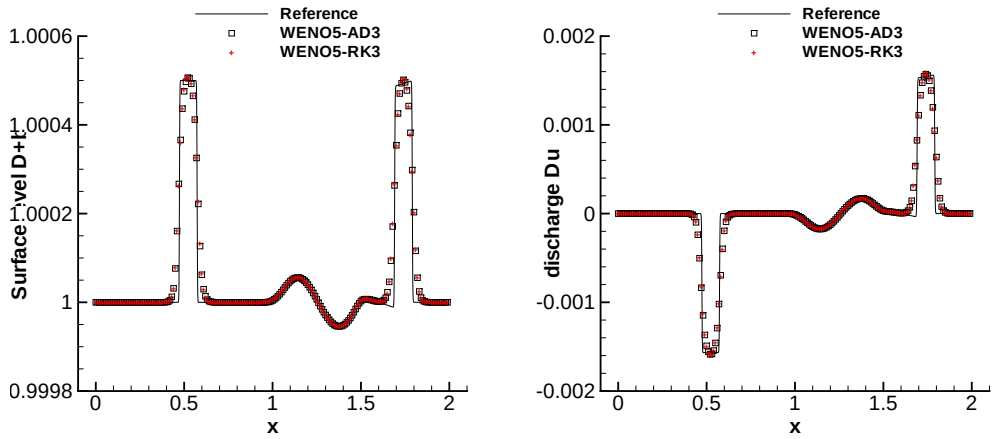

Figure 5: Small pulse for the small perturbation of steady-state water by WENO5-AD3, WENO5-RK3. Left: surface level; Right: discharge.

on resolution. We run 100 times for every program as the CPU time to the small pulse problem, the cost CPU time for WENO5-AD3 schemes is 2.73s, for WENO5-RK3 schemes is 3.45s, while the cost CPU time for WENO5-AD4 schemes is 4.18s, for WENO5-RK4 schemes is 4.63s.

Example 3.5. An two-dimensional accuracy test. To check the numerical accuracy for the two-dimensional shallow water equations we use the same test in [19]. On the unit square $[0,1]\times[0,1]$, the bottom topography is given by

$$b(x,y)=\sin(2\pi x)+\cos(2\pi y),$$

and the initial data are given by

$$\begin{aligned}&D(x,y,0)=10+e^{\sin(2\pi x)}\cos(2\pi y),\\&(Du)(x,y,0)=\sin(\cos(2\pi x))\sin(2\pi y),\\&(Dv)(x,y,0)=\cos(2\pi x)\cos(\sin(2\pi y)).\end{aligned}$$

We take the still water height h as $h=10-b(x,y)$. We compute up to time $t=0.05s$ when there is no shocks in the solution, with 4-periodic boundary conditions. The reference solution is computed with the same scheme and 1600 cells in x-direction and y-direction separately, since the exact solution is unknown.

Table 6: An two-dimensional accuracy test. L^1 errors and numerical orders of accuracy by the WENO5-AD3 scheme.

N	D		Du		Dv	
	L^1 error	order	L^1 error	order	L^1 error	order
25×25	1.189E-2		3.725E-2		9.952E-2	
50×50	1.427E-3	3.06	2.789E-3	3.74	1.338E-2	2.89
100×100	1.021E-4	3.81	1.554E-4	4.16	9.542E-4	3.81
200×200	5.211E-6	4.29	7.306E-6	4.40	4.802E-5	4.31
400×400	2.038E-7	4.73	2.958E-7	4.63	1.847E-6	4.70

Table 7: An two-dimensional accuracy test. L^∞ errors and numerical orders of accuracy by the WENO5-AD3 scheme.

N	D		Du		Dv	
	L^∞ error	order	L^∞ error	order	L^∞ error	order
25×25	9.597E-2		1.145E-1		1.014E-0	
50×50	2.507E-2	1.94	2.261E-2	2.68	2.764E-1	1.88
100×100	4.138E-3	2.60	2.692E-3	3.07	4.201E-2	2.72
200×200	3.435E-4	3.59	1.905E-4	3.82	3.230E-3	3.70
400×400	1.719E-5	4.32	9.807E-6	4.28	1.791E-4	4.17

In Tables 6 and 7, the L^1 and L^∞ errors and orderly accuracy for water depth D, the discharge Du and Dv obtained by using WENO5-AD3 scheme are displayed, where N is the cell number. We can see that the fifth order of accuracy are almost achieved for the WENO5-AD3 schemes.

Example 3.6. Test for the exact C-property in two dimensions. To check the exact C-property in two-dimensional flow over a non-flat bottom, we use the following test case [15, 19], namely the bottom is defined with

$$b(x,y) = 0.8e^{-50((x-0.5)^2+(y-0.5)^2)}, \qquad x,y \in [0,1],$$

and same to the one-dimensional case, the initial water height is defined as $D(x,y) = 1 - b(x,y)$, and the initial velocity u, v are defined as zero. The surface should remain flat. The terminal time is taken as $t = 0.1s$.

Table 8: L^∞ errors for the accuracy for the stationary solution in two-dimensionals, WENO5-AD3 and WENO5-RK3 using N cells.

N	WENO5-AD3			WENO5-RK3		
	D	Du	Dv	D	Du	Dv
100×100	2.22E-14	6.72E-13	1.12E-13	2.22E-14	6.72E-13	8.79E-13
50×50	2.22E-14	3.51E-13	6.15E-13	2.22E-14	3.30E-13	4.21E-13
10×10	4.44E-14	5.40E-14	6.37E-14	2.22E-14	4.27E-14	8.14E-14

We take the still level h as $h = 1 - b(x,y)$. In Table 8, L^∞ errors for the water height D and the discharge Du, Dv for WENO5-AD3 and WENO5-RK3 are presented respectively with different meshes. The results are at the level of $1E-14$, and obviously are round off errors, verifying the exact C-property. The cost CPU time is 1.54s for WENO5-AD3, and 1.73s for WENO3-RK3 when cell number is 100×100.

Example 3.7. Asymmetric break of dam. We consider the sudden break of a dam separating two basins with the surface level of 5m (downstream) and 10m (upstream). The dam breaks asymmetrically at time $t = 0$ when velocity are zero. We simulate the test case until time $t = 7.2s$. The length of the breach is 75m and it starts at $y = 95$. Reflection boundary conditions are applied on all the edges of the domain. Fig. 6 shows the description and the initial conditions of the test case.

The contours of the surface level and velocity vectors computed by WENO5-AD3 and WENO5-RK3 on a meshes with 200×200 cells are shown in Fig. 7. We can see in the figures that the right moving water of upstream from propagate to the downstream up and down, and suction wave propagate to the upstream, two asymmetric spiral vortexes are formed because the great velocity and the reflection of wave on the upper wall on both side of breach. The results by WENO5-AD3 and WENO5-RK3 are similar, and our results are similar to other results presented in the literature greatly, e.g. [1, 6, 15]. The cost CPU time for WENO5-AD3 is 29.9s, for WENO5-RK3 is 34.5s.

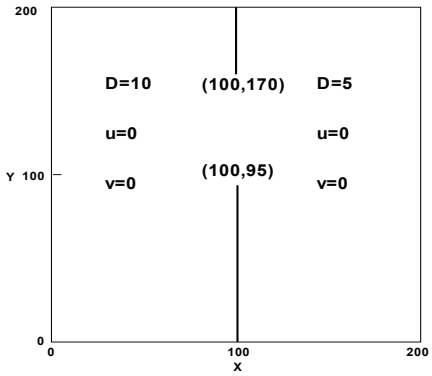

Figure 6: The description and the initial conditions of asymmetric dam break.

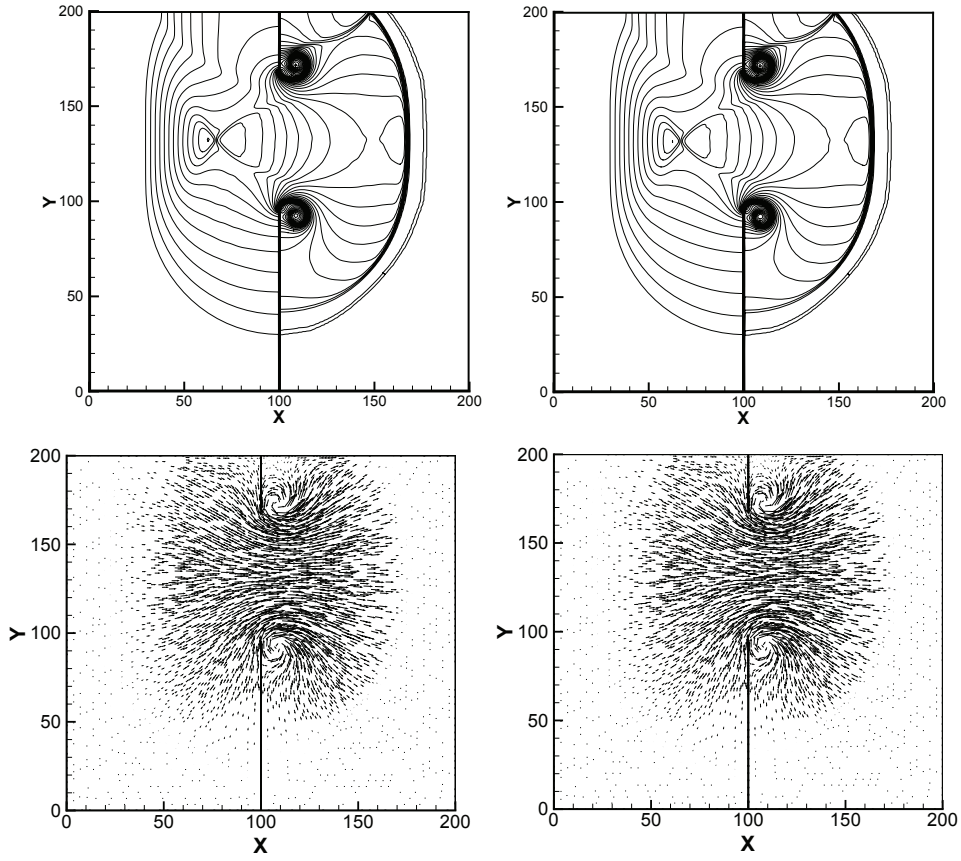

Figure 7: Asymmetric break of dam. Contours of the surface level by WENO5-AD3 (left top); Velocity vectors by WENO5-AD3 (left bottom); Contours of the surface level by WENO5-RK3 (right top); Velocity vectors by WENO5-RK3 (right bottom).

Example 3.8. A small perturbation of steady-state water in two dimensions. This is a classical example to show the capability of the proposed scheme for the perturbation of the stationary state for the two-dimensional shallow water flows [12, 16]. In this case, the bottom topography is given by the function

$$b(x,y) = 0.8\mathrm{e}^{-5(x-0.9)^2-50(y-0.5)^2}, \qquad x,y \in [0,2]\times[0,1].$$

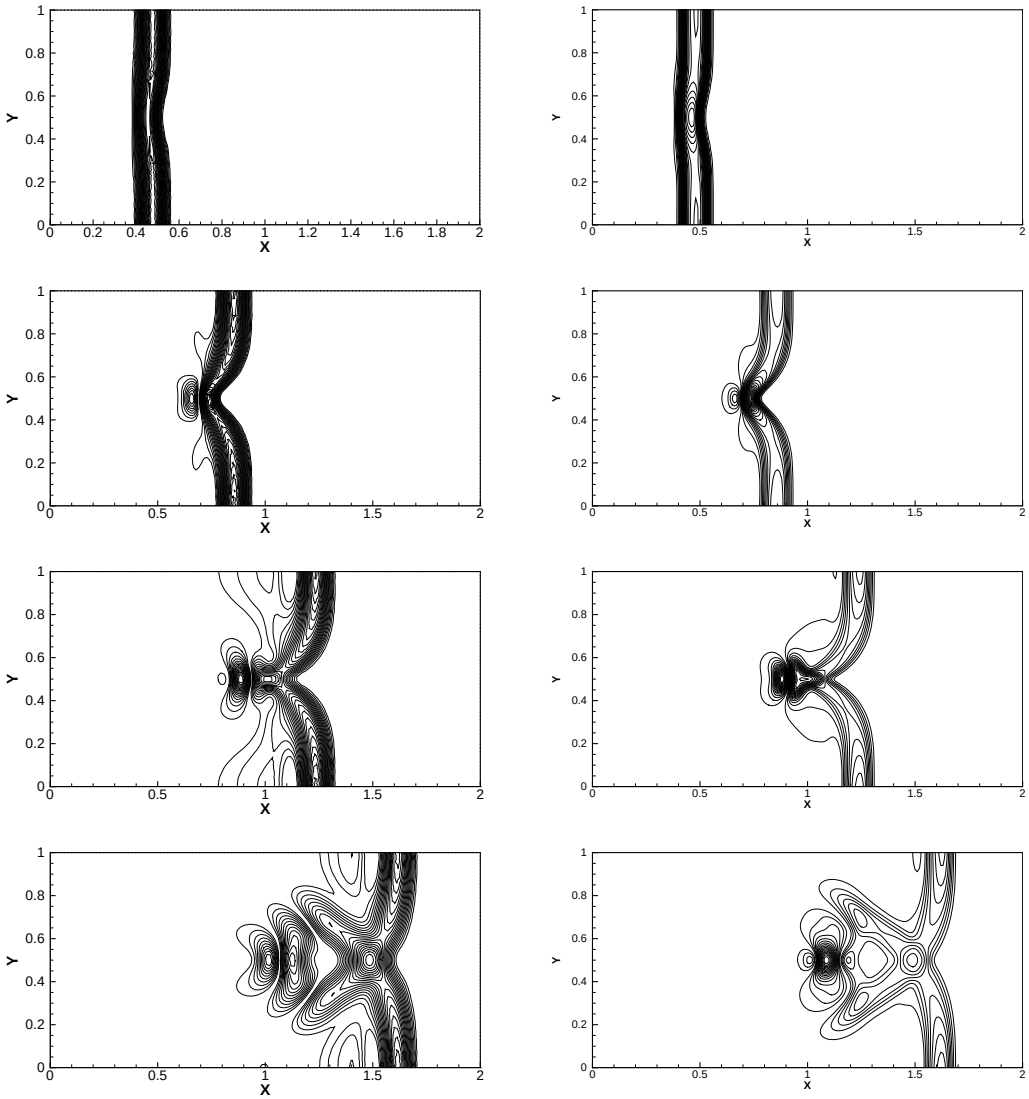

Figure 8: A small perturbation of steady-state water in two dimensions. The contours of the surface level by WENO5-AD3 (left) and WENO5-RK3 (right) at time $0.12s$, $0.24s$, $0.36s$, $0.48s$ (from top to bottom), 30 uniformly spaced contour lines.

The initial surface level and initial velocity are given by

$$D(x,y)=\begin{cases} 1-b(x,y)+0.01, & 0.05\le x\le 0.15,\\ 1-b(x,y), & \text{otherwise,}\end{cases} \qquad u(x,y,0)=v(x,y,0)=0.$$

The absorbing extrapolation boundary conditions of left and right boundary are used, and the reflection boundary condition is used for up and down solid wall boundary.

We take the still water height h as $h=1-b(x,y)$. Fig. 8 displays the right-going disturbance as it propagates the bottom hump on a mesh with 200×100 cells, the contours of the surface level $D+b$ are presented at different time 0.12s, 0.24s, 0.36s, 0.48s. The results are in good agreement with other published results and indicate that the scheme can resolve the complex small features of the flow very well. To the ending time 0.12s, the cost CPU time for WENO5-AD3 is 15.7s, while for WENO5-RK3 is 17.5s, and to the other ending time, the cost CPU time of WENO5-AD3 and WENO5-RK3 maintain almost the corresponding ratio.

4. Concluding remarks

In this paper, we simulate the one-dimensional and two-dimensional shallow water equations with source terms by high resolution finite difference WENO schemes with linear multilevel high order time discretizations. We compare the numerical results with those obtained by finite difference WENO schemes using same order Runge-Kutta time discretizations by addressing CPU time, efficiency and resolution. The numerical results in Section 3 show that the WENO5-AD3 schemes can simulate the flow accurately and catch the stronger discontinuous like WENO5-RK3 in water wave, and the WENO5-AD3 schemes have smaller CPU costs than those needed by the third order Runge-Kutta time discretization. We can see that the cost CPU time of WENO5-AD3 is about 80% of WENO5-RK3 for one-dimensional tests, and about 90% of WENO5-RK3 for two dimensional tests. WENO5-RK4 and WENO5-AD4 cost similar ratio time, and similar resolution. Generally, the implementation of multilevel time discretization is more cost effective than single step time discretization with the same order of accuracy, and multilevel time discretization can make full use of computed information by WENO spatial discretization, so they have higher accuracy, maintain similar high resolution and obtain non spurious oscillatory numerical solutions.

Acknowledgments The research was supported by NSFC 40906048, NSFC 41040042, NSFC 40801200 and Science research fund of Nanjing University of information science & technology 20090203.

References

[1] K. Anastasiou, C. T. Chan, Solution of the 2D shallow water equations using the finite volume method on unstructured triangular meshes, Int. J. Numer. Methods Fluids, 24(1997) 1225-1245.

[2] F. Arĺd'ndiga, A. M. Belda, P. Mulet, Point-Value WENO Multiresolution Applications to Stable Image Compression, J. Sci. Comput., 43(2009) 158-182.
[3] D. Balsara, C. W. Shu, Monotonicity preserving weithted essentially non-oscillatory schemes with increasingly high order of accuracy, J. Comput. Phys., 160(2000) 405-452.
[4] D. Balsara, Divergence-free reconstruction of magnetic fields and WENO schemes for magnetohydrodynamics, J. Comput. Phys., 228(2009) 5040-5054.
[5] Y. Cai, I. M. Navon, Parallel Block Preconditioning Techniques for the Numerical Simulation of the Shallow Water Flow Using Finite Element Methods, J. Comput. Phys., 122(1995) 39-50.
[6] V. Chleffi, A. valaini, A. Zanni, Finite volume method for simulating extreme flood events in natural channels, J. Hydraul. Res., 41(2003) 167-177.
[7] G. A. Gerolymos, D. Sénéchal, I. Vallet, Very-high-order WENO schemes, J. Comput. Phys., 228(1999) 8481-8524.
[8] A. Harten, B. Engguist, S. Osher, S. Chakravarthy, Uniformly high order essentially non-oscillatory schemes, , J. Comput. Phys., v71(1987) 231-303.
[9] A. Harten, S. Osher, Uniformly high-order accurate non-oscillatory schemes, *I*, SIAM J. Num. Analy., v24 (1987), 279-309.
[10] C. Hu, C. W. Shu, Weighted essentially non-oscillatory schemes on triangular meshes, J. Comput. Phys., 150(1999) 97-127.
[11] G. S. Jiang, C. W. Shu, Effecient implementation of weighted ENO schemes, J. Comput. Phys., 126(1996) 202-228.
[12] R. J. LeVeque, Balancing source terms and flux gradients in high-resolution Godunov method: the quasi-steady wave-propagation algorithm, J. Comput. Phys., 346(1998) 146.
[13] X. D. Liu, S. Osher, T. Chan, Weighted essentially non-oscillatory schemes, J. Comput. Phys., 115(1994) 200-212.
[14] J. X. Qiu, C. W. Shu, Finite difference WENO schemes with Lax-wendroff-type time discretizations, SIAM J. Sci. Comput., 24(2003) 2185-2198.
[15] M. Ricchiuto, R. Abgrall, H. Deconinck, Application of conservative residual distribution schemes to the solution of the shallow water equations on unstructured meshes, J. Comput. Phys., 222(2007) 287-331.
[16] B. D. Rogers, Alistair G. L. Borthwick, P. H. Taylor, Mathematical balancing of flux gradient and source terms prior to using Roe's approximate Riemann solver, J. Comput. Phys., 192(2003) 422-451.
[17] C. W. Shu, Essential non-oscillatory and weighted essentially non-oscillatory schemes for hyperbolic conservation laws, In: B. Cockburn, C. Johnson, C. W. Shu, E. Tadmor. Advanced numerical approximation of nonlinear hyperbolic equations. In: A Quarteroni, e ditor. Lecture Notes in Mathematics, vol. 1697. Berlin: Springer, 1998. 325-432.
[18] C. W. Shu, Total-variation-diminishing time discretizations, SIAM J. Sci. and Stat. Comput., 24(2003) 2185-2198.
[19] Y. L. Xing, C. W. Shu, High order finite difference WENO schemes with the exact conservation property for the shallow water equations, J. Comput. Phys., 208(2005) 206-227.
[20] J. Zhu, J. X. Qiu, Hermite WENO Schemes and Their Application as Limiters for Runge-Kutta Discontinuous Galerkin Method, III: Unstructured Meshes, J. Sci. Comput., 39(2009) 293-321.
[21] Y. H. Zahran, An efficient WENO scheme for solving hyperbolic conservation laws, Appl. Math. Comput. , 212(2009) 37-50.